

UNCLASSIFIED

N - 1968

INSTRUMENTATION

**EXPERIMENTS WITH A SLOW NEUTRON VELOCITY SPECTROMETER**

by

France Barnet Berger

1942

University of Illinois

Styled, retyped, and reproduced from copy  
as submitted to this office.

**UNITED STATES ATOMIC ENERGY COMMISSION**  
Technical Information Division, ORE, Oak Ridge, Tennessee  
AEC, Oak Ridge, Tenn., 5-10-50-98--A19867

UNCLASSIFIED

## EXPERIMENTS WITH A SLOW NEUTRON VELOCITY SPECTROMETER\*

By France Barnet Berger

### 1. INTRODUCTION

The absorption of slow neutrons by various nuclei is known to depend on the neutron velocity. Most nuclei show an increasing absorption with decreasing neutron velocity, while many exhibit selective absorption. The slow neutrons used to investigate these effects are obtained by slowing down in a hydrogenous substance the fast neutrons produced in nuclear disintegrations. The velocity of the neutrons for the particular process under investigation must be determined either by a direct method or by an indirect method.

A number of indirect methods have been developed, but these are not of particular concern in this paper. The direct methods, including the method used in the investigation reported here, are based on the determination of the time of flight of the slow neutrons over a known distance.

The first direct method, reported in 1935, was that of Dunning, Pogram, Fink, Mitchell and Segre<sup>1</sup> in which two rotating sets of cadmium-covered sector disks, separated a given distance, serve as modulator and analyzer of the neutron beam.

Alvarez<sup>2</sup> produced bursts of neutrons by modulating the oscillator voltage supply of a cyclotron with 60- or 120-cycle alternating current. The intermittent target current gave rise to neutrons during only a short portion of each cycle. The recording time was likewise short and was at an adjustable time after the neutron burst.

Fertel, Gibbs, Moon, Thomson, and Wynn-Williams<sup>3</sup> obtained neutron bursts by modulating the ion source of a linear accelerator, and the velocity distributions of the neutrons were obtained by photographing the screen of a cathode-ray oscilloscope with the linear sweep serving as the time scale on which the neutron pulses were impressed.

Baker and Bacher<sup>4</sup> modulated the cyclotron arc source and recorded the delayed neutrons by modulating the pulse amplifier in such a manner as to confine its output to the desired time interval.

The velocity spectrometer in this laboratory, as reported by Haworth, Manley, and Luebke,<sup>5-8</sup> has the Illinois linear accelerator as the neutron source, the fast neutron output being controlled by deflecting the ions comprising the beam after they have been accelerated but before they reach

---

\*Thesis submitted in partial fulfillment of the requirements for the degree of doctor of philosophy in physics, in the Graduate School of the University of Illinois, 1942.

the target. The recording was done photographically, following the general plan of Fertel et al.<sup>3</sup> In more recent work carried out in this laboratory, reported by F. Gillette<sup>9</sup> and in this paper, the photographic method of recording has been superseded by an automatic method of recording which possesses some advantages over the previously described velocity spectrometers.

The author has investigated the absorption of slow neutrons in mercury as a function of neutron velocity. The probable existence of a resonance in the absorption of neutrons in the thermal energy range has been reported for this element.<sup>10,11</sup> The results of Baker and Bacher<sup>4</sup> and Luebke<sup>6</sup> indicate that if such a resonance exists in the part of the velocity spectrum where it is reported to exist, the apparatus in this laboratory would probably resolve it.

The author has investigated also the distributions in velocity of the neutrons emitted by paraffin-wax slow neutron sources of different temperatures. A knowledge of these velocity spectra is valuable in helping to evaluate the results of experiments in which sources similar to those investigated are employed.<sup>10,12</sup>

The information that can be obtained from any slow neutron velocity spectrometer experiment is limited by the resolution of the apparatus. The shorter the duration of the neutron pulse and the shorter the detecting time intervals, the better defined is the velocity corresponding to the average time of flight. It can readily be seen, also, that the greater the distance from the source to the detector, the better is the resolution, because under these conditions not only are the finite thicknesses of the detector and of the source a smaller fraction of the distance traversed, but also the dispersion of the neutrons in the beam is greater. Unfortunately, however, so far no fast neutron source has been employed of intensity sufficient to enable experiments to be performed under conditions such that the resolution corrections are negligible. There must be, therefore, a compromise between resolution and intensity and a correction for the resolution in the best manner possible. The author, accordingly, has examined the characteristics of the source employed and has attempted to correct the observations for the resolution effects.

## 2. APPARATUS

The construction and operation of the Illinois linear accelerator have been described,<sup>5-7</sup> and inasmuch as a detailed knowledge of this material is nonessential to an understanding of the present experiments, these will not be considered in this paper.

### Circuits

Figure 1 is a block diagram of the modulating, detecting, and analyzing circuits. The elements not previously described were designed and constructed by L. J. Havorth and F. W. Gillette.<sup>9</sup>

Taken as a unit, the circuits perform the following functions: Once every cycle at a given frequency, called the "cycle frequency," the voltage on the beam deflecting plates is removed for a time generally short compared to the cycle period, and the deuteron beam impinges on the heavy-water ice

target, producing fast neutrons. The neutralizing square wave of voltage will be referred to as the "beam pulse." Some of the neutrons, after the slowing down in the paraffin surrounding the target, diffuse out and traverse the distance to the detector and arrive at times depending on their respective velocities. Pulses from the detecting ionization chamber, after suitable amplification, sorting, and sharpening, are sent into the analyzer. This device causes the pulses to be recorded on one of ten Cenco counters. These counters are sensitive, one after the other, each for a given length of time which, under most operating conditions, is short compared to the cycle period. The sensitive time of the first of the counters is initiated, after a known time lapse or "delay" if desired, by the beam pulse. Thus the pulse produced by each neutron is recorded on the Cenco counter that is sensitive when the neutron in question arrives at the detector. The time of flight of each neutron is determined, therefore, within bounds which depend on the beam-pulse duration and on the sensitive period of each interval.

A brief description of the various circuit elements is given for the sake of completeness. The master oscillator operates at a frequency of 100 kilocycles, the crystal oscillator serving to keep the frequency constant. The sinusoidal output of the master oscillator is fed into the oscillator sharpener which gives an output suitable for tripping the 10-stage scaling circuit. The purpose of the scaler is to make available pulses of different fixed frequencies corresponding to periods of 20, 40, 80, 160, ..., ...,  $2^9 \times 10$ , and  $2^{10} \times 10$  ( $= 10,240$ ) microseconds. The signals from this unit control the timing of the beam pulse and the counters.

The delay, the delay follower, and the dummy circuits serve to synchronize the initiation of the beam pulse and the initiation of the sensitive time of the first counter. These may be made to start simultaneously, or either one may be delayed with respect to the other by any time up to half the cycle period. The master pulse and the beam pulse circuits supply the neutralizing voltage to the deflecting plates. The length of the beam pulse is continuously variable from 30 to 1000 microseconds.

The analyzer utilizes the basic features of the coincidence circuit and of the scaling circuit. Corresponding to each of the 10 time intervals is a coincidence circuit. One of the coincident pulses is a square wave, the duration of which is the sensitive time of one counter; the other is the incoming neutron pulse from the  $\text{BF}_3$  ionization chamber. The square wave comes from the corresponding one of ten altered scale of two elements which are connected, one grid of each unit leading to the "time scale" signal and the other grid coupled to the plate of the preceding stage. Once the first unit is tripped by the signal synchronized with the beam pulse, each time-scale pulse trips the succeeding stage.

#### Detector

A parallel-plate ionization chamber filled with an atmosphere of boron trifluoride is used as the neutron detector. In it are three 1/16-in. aluminum plates, each 19 cm in diameter and spaced 2 cm apart, that are mounted on lucite insulators. The neutrons entering the sensitive region of the chamber must first penetrate the 1/32-in. brass faceplate and 1 cm of the  $\text{BF}_3$  as well as either one or two of the aluminum plates. When  $\beta^{10}$

captures a slow neutron, it emits an alpha particle and is thereby transformed into  $\text{Li}^7$ ; positive ions formed by the ejected particles are collected on the middle plate. This action causes a positive pulse to feed onto the grid of the tube in the first stage of a four-stage linear amplifier. Optimum performance of a newly filled chamber was generally obtained with a collecting voltage of about 1500. Owing probably to air and water vapor leaking into the chamber, the optimum collecting voltage gradually drifted downward; for some fillings it drifted to as low as 375 volts. Surprisingly enough, the efficiency of the detector did not change greatly with the drift in optimum voltage over most of its range. The absorption of the sensitive region of the chamber varies from about 10 per cent for neutrons with a velocity of 1.5 km/sec to about 1 per cent for those with a velocity of 20 km/sec; therefore it can be assumed that for the range of velocities covered in the investigation the detector is "thin." The output of the linear amplifier is fed into a discriminating circuit which gives an output pulse only if the size of the input pulse exceeds some (adjustable) critical value. This eliminates most of the counts that would be recorded because of the "noise" background of the amplifier. The output of this discriminating circuit is sharpened into a pulse of about 8 microseconds duration before being fed into the analyzing circuit, thereby minimizing the number of pulses that will be recorded not only in the proper interval but also in an adjacent interval.

#### Geometry

The geometrical arrangement of the source, detector, and shielding is shown in Fig. 2. The chamber is surrounded on all sides except the front by 0.5 mm of cadmium, several centimeters of borax, and then by more cadmium. The beam is collimated by the cadmium-lined and borax-filled tubes shown in the figure. Most of the data were taken with arrangement A of Fig. 2 in which the distance from the center of the chamber to the paraffin surface is 248.5 cm. The absorbers were placed in the position X-X. With arrangement B of Fig. 2 the absorber is placed close to the detector (about 10 cm closer than shown in the figure). The source position, not well defined as in the previous case, is taken at the dotted line. The source to detector distance for this arrangement is then 129 cm. The position of the monitoring counter is shown in both diagrams.

The source illustrated in part A consists of a paraffin cube 1 $\frac{1}{2}$  cm on an edge. A second source, Arrangement B, shown in Fig. 2, consists of half of the cube of part A and of three soft-glass thermos flasks, each containing 1 lb of paraffin cooled with a dry-ice - alcohol mixture, 50 per cent alcohol by volume. The half-life of delayed emission neutrons from this source is 80 microseconds. The walls of the flasks were found to be almost completely transparent to slow neutrons. A third source arrangement is illustrated in Fig. 3. The special apparatus was constructed to enable cooling of a block of paraffin with liquid air to a very low temperature. The space between the outer casing and the paraffin is evacuated to cut down the heat flow by conduction and convection to the cold interior. Most of this Dewar vessel is constructed of brass; however, the faceplates on the outer can are 20-mil iron, the section of tubing that supports the paraffin can is German silver, and the liquid-air cavity, the vanes extending throughout the wax, and the inner faceplates are copper. A thermocouple junction is placed at C. The paraffin was cooled with dry ice and alcohol to about  $-30^{\circ}\text{C}$

to conserve liquid air. Liquid air was then continuously forced into the cavity from a 4-liter glass Dewar flask through a rubber hose by compressed air, a slit rubber hose in the compressed-air line serving as a safety valve. About 6 hr (and 8 liters of liquid air) are required for the thermocouple to indicate that the temperature has reached a steady-state value. The minimum temperature obtainable depends on the pressure of the gas in the "evacuated" space, being  $-140^{\circ}\text{C}$  for a pressure a little lower than  $10^{-3}$  mm Hg. Once the paraffin reaches the minimum temperature, about 1 liter of air per hour suffices to maintain the temperature constant. The arrangement has the very great disadvantage, over and above that of requiring much liquid air, of demanding continuous attention.

The absorber used in the determination of the cross section of mercury consists of 341 g of liquid mercury contained between 1/32-in. aluminum sheets. Aluminum spacers are used around the edges, and 13 small spacers are used throughout the area of the absorber to limit the variation in wall separation due to hydrostatic pressure. The thickness of the assembled and filled absorber was measured at many points, and the magnitude of the error introduced in the calculated value of the cross section by assuming a uniform thickness equal to the average thickness was estimated. As the results indicate divergences of about 1 per cent or less, corrections for this effect were not made. The absorber areas occupied by the small aluminum spacers are covered with cadmium, and all the data have been corrected for the consequent reduction in beam area (1.3 per cent). The absorption of the aluminum container was found to be negligible, which would be expected since the accepted value of the absorption coefficient of aluminum for slow neutrons is small. The area occupied by the mercury was found to be 509 sq cm, giving an average absorber thickness of  $0.670$  g/sq cm, or  $2.02 \times 10^{21}$  atoms/sq cm, this value probably being correct to within one-third of 1 per cent.

#### Calibration

During each day's run, the frequency of the crystal oscillator, which serves as the standard of time measurement, was checked several times by beating its output against the carrier frequency of a suitably chosen radio station. It was never found to be off by more than a few cycles per second.

The beam-pulse off time, which is continuously adjustable, was set by superimposing the signal from the beam-pulse generator and the signals from the time-scale circuit on a 6-in. oscilloscope screen. The time settings could be made accurate to within 3 microseconds.

At frequent intervals while taking data the operation of the analysing circuit was checked by observing the position of the sensitive time of each interval on the oscilloscope screen. Only rarely did any data have to be discarded because of instability of the circuits.

It is important in obtaining velocity distributions that each of the counting intervals be equally long. This point was checked several times by two independent methods. One method was to record random counts on the ten Cenco counters until thousands of counts were recorded on each. This was done with the linear accelerator as a source of neutrons and also with radium-beryllium in paraffin as a source. No deviations from equality of time intervals were found that were larger than expected from statistical considerations. To check on possible overlap of the intervals, one of the

counters was used as a "totaler." It was found that a small percentage (less than 1 per cent for 160-microsecond intervals) of the counts get into two adjacent time intervals; since the overlap is slight, its effect was neglected in working up the data. The second method was to feed in regular pulses synchronized with the time-scale frequency. Once the Cenco counters were properly adjusted, no significant variations in their recordings were subsequently observed. In some cases data were taken with eight counters spanning the beam-pulse period (Fig. 4, Part E); under such circumstances counters 9 and 10 were sensitive during the same time intervals as were 1 and 2. The discrepancies between the counters recording for the same time intervals were too small to be significant.

There are various delays which must be considered before the data can be correctly interpreted. They are

- $d_1$ , the time elapsed after the beam pulse goes on until deuterons hit the target
- $d_2$ , the time taken for fast neutrons to slow down and to diffuse out of the paraffin
- $d_3$ , the time of flight from paraffin to chamber, the time sought in these experiments
- $d_4$ , the collecting time of the ions in the ionization chamber
- $d_5$ , the delay in the amplifier
- $d_6$ , the time from the start of the output pulse of the amplifier to the firing of the discriminator thyatron
- $d_7$ , the delay in the pulse sharpener
- $d_8$ , in the case of the cylindrical BF<sub>3</sub> counter, instead of  $d_4$ ,  $d_5$ , and  $d_6$  there is  $d_8$ , the delay in the counter and counter circuits.

The delay  $d_1$  was previously measured for the linear accelerator<sup>5</sup> and found to be less than 2 microseconds. The over-all delay was determined in the following way. The ionization chamber was moved close to the target, all paraffin was removed, and, in addition, the chamber was completely surrounded by cadmium to exclude slow neutrons. The detector time intervals were set at 40 microseconds and the beam-pulse time of 160 microseconds was adjusted to overlap intervals 5 to 8 (Fig. 4, Part B). Owing to the delays, the fast neutrons (which come in almost a square wave) do not come in just the intervals 5 to 8 but are observed in full intensity in intervals 7, 8, and 9 and partially in intervals 6 and 10. This indicates a delay of between 40 and 80 microseconds. To make full use of the observed data, the counts for each combination of four successive intervals is summed and plotted against the overlap time, or the time from the beginning of the beam pulse to the end of the sensitive time. As the background count was found to be very low and apparently uniform, the missing intervals (11 to 16) are assumed to have the average background count. The results for one discriminator setting and for 635 volts on the collecting plates are shown in Fig. 4. The fact that the crest of the curve and the descending intercept yield practically the same values for the delay as the intercept on the ascending side does indicate that no appreciable number of slow neutrons could have been reaching the chamber. Data taken with a quite different discriminator setting gave practically the same delay time, so for the range of settings used in the experiments, a value of  $55 \pm 5$  microseconds may be assumed. Knowing this value, which is a measure of the sum  $d_1 + d_4 + d_5 + d_6 + d_7$ , makes it unnecessary to know these delays separately. In the treatment of all data this delay has been taken into consideration.

The delay  $d_2$  is estimated from the source growth-decay curves shown in Fig. 5. For even the fastest neutrons (Cd absorber data) there is a delay of about 10 microseconds before the detector records any neutrons. It is to be pointed out that the curves must not be drawn through the experimental points, but they must be drawn in such a way as to include the same area as the histogram and still be approximately exponential (this point is discussed in reference 5). The nature of these curves is discussed later in this paper. Inasmuch as  $d_7$  or  $d_8$  would not be expected to be appreciable, this 10 microseconds is the value ascribed to  $d_2$ . This delay is taken into consideration in the treatment of the data by incorporating it into the source function used in correcting for resolution.

### 3. EXPERIMENTAL PROCEDURE AND REDUCTION OF DATA

The detecting equipment was turned on and allowed to warm up for 1/2 hr or longer before taking data. During this time the linear accelerator beam was adjusted to give the largest beam current obtainable (about 10 microamperes when the beam was on the target one-sixteenth of the time). Fine adjustments were then made to get the largest ratio of beam current with the beam pulse turned on to the beam current with the beam permanently deflected. This ratio was generally about 10 to 1. However, the production of neutrons per unit current decreases rapidly with increasing current; therefore the corresponding ratio of neutron intensities was only 5 or 6 to 1.

The runs indicated in Table 1 were taken in fixed sequence.

Table 1

Absorber	Time, sec	Beam pulse	Notation
None	600	On	$N_o$
None	150	Off	$N_o'$
Thick boron + Cd	600*	On	$N_b$
Thick boron + Cd	150	Off	$N_b'$
Mercury†	600	On	$N_m$
Mercury†	150	Off	$N_m'$

\*When the sensitive intervals were delayed with respect to the beam pulse, 150-sec runs were taken.

†Some data were taken without mercury runs in the sequence for the velocity distribution work.

The "off" runs are shorter than the "on" runs; since each time interval is of the same length, each off run gives 10 independent background determinations, while for the "on" runs, each time interval is a measure of a different quantity. Before and after each set of runs the natural background of the chamber was determined with the beam accelerating voltage off. This chamber background was generally very small (1 count per interval per 100 sec, or less) and hence could be neglected. However, on some days this background was appreciable and was taken from all six of

the observations indicated in Table 1 before any further calculations were made. This background was assumed to have a magnitude directly proportional to time. The observed quantities, with chamber background subtracted, have the following interpretations:

$N_b$  gives a measure of the neutrons that go around about the collimating tube owing both to the pulses and to the stray or undeflected component of the beam. The thick boron plus cadmium (5 mm  $B_4C$  + 0.5 mm Cd) absorbs practically all the neutrons going down the tube.

$N_b$  or  $N_m^i$  gives a measure of the neutrons that go down the collimating tube and of those that go around the tube owing to just the stray beam.

$N_b^i$  gives a measure of the neutrons that go around the tube owing to the stray beam alone.

Before these various backgrounds can be applied as corrections to the observed number  $N_o$ , they must be normalized to correspond to the same integrated source intensity. To make this possible, a monitor, consisting of a boron trifluoride - filled cylindrical counter, was placed about 1 cm from the surface of the paraffin cube on the side opposite the collimating tube, and it was not moved during any day's run. Its output, scaled by 8, was recorded on a Cenco counter. Let  $M_o$ ,  $M_o^i$ , etc., represent the monitor counts associated with the runs which yield the numbers  $N_o$ ,  $N_o^i$ , etc., respectively. Further, let  $N_o^*$ ,  $N_o^{*i}$ , etc., represent the corresponding normalized values of these numbers. Then, taking  $N_o^* = N_o$  as a basis of comparison,

$$N_b^* = N_b (M_o/M_b)$$

and

$$N_m^* = N_m (M_o/M_m)$$

To correct the off observations, the plausible assumption must be made that, although the beam current varies slowly with time, the average beam current during the time of the off runs is the same as the average beam current (and hence average off neutron intensity) during the time of the on runs. Making this assumption, R, the ratio of on monitor counts to off monitor counts per unit time, was calculated. The off observations were normalized using the relations

$$N_o^{*i} = N_o^i M_o / (R M_o^i)$$

etc.

The net values were then calculated as follows:

$$N_o(\text{net}) = (N_o^* - N_o^{*i}) - (N_b^* - N_b^{*i})$$

$$N_m(\text{net}) = (N_m^* - N_m^{*i}) - (N_b^* - N_b^{*i})$$

and the cross section  $\sigma_1$  for neutrons arriving in any time interval  $i$  was computed from

$$N_m(\text{net})_i = N_o(\text{net})_i e^{-\sigma_1}$$

where  $\sigma_1$  is the number of mercury atoms per square centimeter of absorber. As pointed out in the previous paragraph, the off runs give, on the average, the same number of counts in each interval; therefore average of the values

obtained in the 10 time intervals was used in carrying out the above operations.

It was found that the value  $N_0^2$  was about half as large as was  $N_0^1$  for the first 160-microsecond time interval after the deuteron pulse went off. In the second and third intervals, the value of  $N_0^2$  decreased considerably, and from the 4 to 16 time intervals its value was constant and only slightly larger than the value of  $N_0^1$ . Baker and Bacher<sup>4</sup> observed the same behavior of this background and, reasonably enough, attributed it to neutrons which are slowed down gradually by being scattered around the room before entering the detector. This interpretation is suggested also by the author's observation that borax and cadmium shielding around the detector were very effective in reducing this background, while placing these absorbing substances, which are relatively transparent to very fast neutrons, around the source had practically no effect.

#### 4. RESULTS

The growth and decay in time of the neutron intensity at the source was measured with a cylindrical boron trifluoride counter placed 4 cm from the face of the paraffin block (Fig. 2C). To gain some idea of how this growth and decay depends on the neutron velocity, various absorbers were placed between the paraffin and the counter. The pertinent data are given in Fig. 5 and Tables 2 and 3. The curves in Fig. 5 are normalized to the same integrated intensity.

Table 2

Curve	Total counts	Detector intervals, microseconds
A	9567	40
B	4033	40
C	3430	40
D	2658	40
E	1379	40
F	7824	40
F	8763	20

Table 3

Absorber	Substance used	Atoms/sq cm of absorber	Container walls
Thin boron	B <sub>4</sub> C	1.00 x 10 <sup>21</sup>	1/16-in. Al
Mercury	Hg	2.02 x 10 <sup>21</sup>	1/16-in. Al
Manganese	Mn	6.45 x 10 <sup>22</sup>	1/16-in. Al
Thick boron	B <sub>4</sub> C	1.04 x 10 <sup>22</sup>	1/16-in. Al
Cadmium	Cd	2.6 x 10 <sup>21</sup>	None

The first three absorbers listed have approximately the same transmission characteristics.<sup>6-9</sup> These curves will be discussed in detail in connection with the resolution of the apparatus.

The values of the cross section of mercury for the neutrons arriving in each time interval are plotted against the number of the interval in Fig. 7. The small circles are the values calculated from the data taken at a distance of 248.5 cm. These data were taken with a sensitive time for each counting interval of 160 microseconds, a cycle period of 2560 microseconds, and a beam pulse of 160 microseconds duration (Fig. 4C and D). Most of these data were taken using the first 10 intervals after the beam-pulse interval (Fig. 4C). Some data were taken with the last 10 intervals of the cycle as the sensitive ones (Fig. 4D), but the results of only intervals 11, 12, and 13 are plotted; the results for the preceding intervals are in agreement with the data plotted, and in intervals 14 and 15 there was not enough intensity to give meaningful results. The numbers along the top abscissa scale of Fig. 7 correspond to the 160-microsecond intervals; the numbers along the second abscissa scale (labeled T) give the time in microseconds after the beam pulse went on. The third scale (labeled  $T_{av}$ ) gives the median time of flight of the neutrons arriving at the detector, with no absorber in the beam, at any time indicated in the second scale. Scales four and five give the velocities in kilometers per second and the energies in electron volts corresponding to the median times of flight given in scale three. Although this method of calculating the energy and velocity to be associated with a given time interval does not completely take the resolution effects into consideration (see Sec. 5), it gives more meaningful values than a calculation based on the T (the 2d) scale would give. The data plotted as dashes in Fig. 7 were taken with a source to detector distance of 129 cm (Fig. 2B), using the same circuit settings as for the above data and with the first 10 intervals recording (Fig. 4C). The time of flight measured from the beam-pulse off time was reduced to 248.5 cm before plotting. The velocity and energy scales of Fig. 7 are based on resolution considerations peculiar to the 248.5 cm data and they are, therefore, applicable to the 129 cm data in only an approximate way. The vertical lines through the points represent the mean statistical errors of the observations.

The results of the investigation of the sources at different temperatures are given in Fig. 6. The curve with the sharpest maximum (labeled A) represents the detector response for the paraffin cube at room temperature. Curve B was obtained using the soft glass Dewar source, the temperature of the paraffin facing the detector being about 200°K. Curve C is a plot of the detector response to the neutrons emerging from the metal Dewar source (Fig. 3) cooled to approximately 135°K. The ordinates for the three curves are adjusted so that there is the same area under each one. The data for all three of these curves were taken at the 248.5 cm distance, using a beam pulse of 160 microseconds duration and a cycle frequency corresponding to 2560 microseconds. For the room-temperature source and for the dry-ice source, 160 microseconds was the detector time employed (Fig. 4C and D), and for the coldest source, times twice as long (Fig. 4E) were used. There is an appreciable number of neutrons slow enough to be detected more than a cycle period after emission. The data as plotted in Figs. 6 and 7 have been corrected for the contribution of these neutrons. The mean statistical errors are indicated on some of the points.

## 5. RESOLUTION OF APPARATUS

The detector response plotted as a function of time of flight of the neutrons cannot in any simple manner be converted into a curve representing the velocity distribution of the neutrons in the beam. The reasons for this are as follows: (a) Each counter records all counts coming in a finite time interval; therefore the data obtained should be plotted as a histogram. (b) The neutrons leave the source each cycle during a length of time that is not small compared to the time of flight. In any small time interval at the detector, therefore, neutrons with velocities within a certain rather large velocity range are arriving. In order to obtain the true velocity distribution of the neutrons, the effects of these factors must be taken into consideration.

A smooth curve  $D(t)$  was drawn over the experimental points in such a way that the area under the curve in each time interval was equal to the area of the corresponding element of the histogram. Since there is no reason to expect any fine structure in the velocity distribution, this procedure compensates for the first effect mentioned above.

The effect on the observations due to the spread in time of the emission of neutrons from the paraffin is much more difficult to evaluate. Baker and Bacher<sup>4</sup> discussed the problem in considerable detail and developed a method of correcting the data obtained at the high-velocity end of the neutron spectrum. The present experiments, however, are carried out with practically the entire slow neutron spectrum; therefore the simplifying assumptions that must be introduced in order to use the method of Baker and Bacher would not be justified.

Fundamentally, the problem of finding the actual number of neutrons, as a function of time of flight, from the observed data  $D(t)$  amounts to finding a solution to the integral equation

$$D(t) = \text{const.} \int_{v = d/t}^{v = \infty} S(t - \frac{d}{v}, v) F(v) dv$$

where  $S(t, v)$  is the function which represents the intensity of the source as a function of time and of neutron velocity  $v$ .  $F(v)$  is the velocity distribution  $N(v)$  multiplied by  $B(v)$ , the efficiency of the detector to neutrons of velocity  $v$ . The source to detector distance is represented by  $d$ . Since  $S(t, v)$  is zero for  $t < 0$ , the lower limit above might just as well be  $v = 0$ . The method used to solve this equation is an approximate numerical one in which the integral is replaced by a sum. The numerical work is simplified if the integral is first transformed to

$$D(t) = \text{const.} \int_0^{t/d} S(t - \frac{d}{v}, v) F'(1/v) d(1/v)$$

in which  $F'(1/v) = v^2 F(v)$ .

In outline, the method of solving the problem is:

- (1) From the curves of growth and decay of the neutron intensity just outside the paraffin block, as observed with various absorbers placed in front of the detector, an expression is obtained for  $S(t, v)$ .
- (2) A velocity distribution as seen by the detector  $F'(1/v)$  is assumed. Using this  $F'(1/v)$  and the function  $S(t, v)$  of part (a), the detector response  $D(t)$  is calculated by an approximate numerical method. From a comparison of the calculated and the observed detector response curves, a second "guess" for the velocity distribution is made, and the calculations are repeated. This process of successive approximations is continued until the true velocity distribution is obtained to the degree of accuracy desired.
- (3) The effect of resolution on the cross-sectional measurements is evaluated indirectly. Using the results of (b), the velocity distribution of the neutrons after passing through a  $1/v$  absorber is calculated. This in turn is used to calculate the detector response that would be expected with the absorber in the beam. The values of the logarithm of the reciprocal transmission for each time interval are then calculated (solid line of Fig. 7). Any divergence of the observed ratios from these calculated ratios indicates departure from the  $1/v$  law assumed for the calculations. Had any very great departures from the  $1/v$  law been found, this procedure would have been inadequate.

The details concerning step 1 are as follows. A boron trifluoride counter was placed with its center 4 cm from the face of the paraffin cube, as illustrated in Fig. 2C. With the Cenco counters each sensitive for 40 microseconds and with the beam pulse lasting for 160 microseconds (Fig. 4A), the growth and decay curves of the neutron intensity were determined. With no absorber present, the growth and decay both are almost exponential curves of half-life about 60 microseconds. However, when  $1/v$  absorbers of various thicknesses are placed over the surface of the paraffin block, the observed growth and decay are not of the simple exponential forms (the departure from these forms increases with increasing absorber thickness). The forms of these curves, which are plotted in Fig. 5, can be explained by assuming that they are sums of exponentials of different decay periods. As stated by Baker and Bacher,<sup>4</sup> the cascading neutrons can be expected to come into equilibrium in a very short time (order of 10 microseconds), but the thermal neutrons take much longer to reach a steady-state condition. This fact and the fact that thick  $1/v$  absorbers transmit the faster neutrons preferentially lead to the belief that the observed source intensity curves can, indeed, be interpreted as suggested above. It might be mentioned that a family of curves obtained using the source shown in Fig. 3 (at 300°K) show a behavior very similar to the family shown in Fig. 5. The half-life with no absorber is 70 microseconds at room temperature and 80 microseconds at 170°K.

In order to arrive at any very definite conclusions concerning the observed source curves, the velocity distribution of the emitted neutrons should be known, but, on the other hand, in order to get the velocity distribution the source function must be known. Luebke<sup>6</sup> obtained a detector response curve under conditions very similar to those prevailing in the present case. He and the author calculated a velocity distribution from his data, assuming an exponential source function of half-life 50 microseconds independent of velocity. Anticipating that this distribution would not differ too greatly from that being sought, it was used in the following three ways the problem was attacked.

1. A velocity  $v_1$  was sought such that if it was assumed that all neutrons in the distribution with  $v$  greater than  $v_1$  decay with a short period (10 microseconds) and all those with  $v$  less than  $v_1$  with a long period (60 microseconds), then the observed curves could be matched. It was found that a different  $v_1$  had to be chosen to fit each of the observed curves; therefore it must be concluded that no such division of the velocity distribution into two groups is adequate to explain the facts.

2. If a Maxwellian distribution is fitted to the slow side of the observed velocity distribution, then the Maxwellian falls below the observed curve on the fast side. The assumption was made that all the neutrons in this excess distribution decay rapidly and that the neutrons of the Maxwellian distribution decay with a long period, but no one Maxwellian (i.e., no one temperature) sufficed to explain all the observed data.

3. A function relating half-life of decay to neutron velocity was assumed, and by approximate numerical integration the detector response was calculated (i.e., the integral equation given above was solved for a very small value of  $d$  using the "Luebke  $F(v)$ "). A reasonably close fit to the data was found after several trials. The results are not too sensitively dependent on the function  $S(t,v)$  chosen, but it is felt that the rough results obtained are perhaps as good as can be obtained with the data available. The whole problem of the interpretation of the observed decay curves is very greatly complicated by the fact that neutrons may enter the detector after passing through the absorber at a very large angle to the normal.

In performing the numerical integration to get the velocity distribution, the summation intervals were taken 40 microseconds apart, and in Table 4 the values of the half-life of growth and decay based on the results of method 3 were used.

Table 4

$v$ , km/sec	Half-life, microseconds
0 to 3.5	77
3.5 to 5.0	40
5.0 to 6.7	21
6.7 to $\infty$	10

These exponential curves for the various velocities were normalized by assuming the same saturation value for the intensity in each case. As a result, each curve represents the same integrated intensity. Since the velocity distribution sought is an average distribution over the whole neutron pulse from the source, this is a proper assumption to make. The behavior of the computed detector response function is fortunately rather sensitive to slight alterations of the  $F(1/v)$  over which one is integrating. The final curve obtained for  $F(1/v)$  (the velocity distribution in the beam as seen by the boron detector plotted against  $1/v$ ) has a sharper maximum than the corresponding curve obtained from the analysis as carried out with Luebke's data.

This difference is due to the fact that different functions  $S(t, v)$  were assumed in performing the two analyses. Since

$$F(v) dv = F'(1/v) d(1/v)$$

we have

$$F(v) = F'(1/v) / v^2$$

Using this transformation, the present  $F'(1/v)$  and the "Luebke  $F'(1/v)$ " have been converted into the relative number versus velocity plots shown in Fig. 8, being curves I and II, respectively. It is to be emphasized that these curves represent the velocity distribution in the beam as seen by the boron detector. However, since the detector is thin and the boron cross section goes as  $1/v$  reference (6), the detector response function  $B(v)$  is very approximately equal to  $1/v$ ; therefore, the true velocity distribution in the beam  $N(v)$  could easily be obtained from the curves given. If the usual assumption is made that the number of neutrons in the beam within a given small velocity range is proportional to  $v$  times the corresponding number inside the paraffin, then the curves in Fig. 8 may be thought of as representing the velocity distribution of the neutrons inside the paraffin. Maxwellian distributions for  $300^\circ\text{K}$  and for  $400^\circ\text{K}$  are represented in the same figure for comparison.

The curve on which the experimental cross-sectional points would be expected to fall if the  $1/v$  law is satisfied is the solid line in Fig. 7. The dip in the curve is at first thought surprising, but its origin can be explained qualitatively. If the source emitted neutrons during only a time short compared to any times of flight measured, an ideal curve for cross section vs. time of flight would be obtained from the data. Now consider the effect of the decay tail on the observed number of neutrons arriving at a time corresponding to a velocity less than that at the maximum of the distribution curve. Those neutrons emitted after the deuteron pulse which arrive at the detector at the given time must be those with greater velocities than those arriving that were emitted during the deuteron pulse. These faster tail neutrons will not be so strongly absorbed as the slower ones, hence a greater fraction of the incident neutrons will be transmitted than in the ideal case. This effect will make the experimental cross-sectional values lie below the ideal values, and the effect can be seen to be the greatest in the velocity range where the curve  $F'(1/v)$  is steepest, since it is there that the faster neutrons are relatively more abundant. On the high-velocity side of the curve the effect is still in the same direction, but it is much smaller. In the case of the data taken at the 129 cm distance, the resolution is poorer, and from the qualitative argument already given the cross sections calculated from these data would be expected to lie below the values obtained from the 248.5 cm data. This tendency of the experimental points is observed. Detailed calculations were not made with these data which were taken primarily for the purpose of seeing whether the  $1/v$  law seemed to extend to the lower velocities.

## 6. DISCUSSION OF RESULTS

The data for the cross section of mercury indicate that for velocities from about 1 km/sec to about 20 km/sec the  $1/v$  law holds and, more specifically, that the cross section

$$\sigma = (1180/v) \times 10^{-24} \text{ sq cm}$$

where  $v$  is measured in kilometers per second. This is indicated by the fact that the observed data for the 248.5-cm distance fall rather nicely on the solid line in Fig. 7 which was calculated by taking into account the resolution of the apparatus and on the assumption that the above expression for the cross section is true. The scattering cross section is assumed to be negligible in comparison to the capture cross section over the velocity range studied. If this assumption were not justified, the ordinates corresponding to the first few time intervals (Fig. 7) would be expected to lie above the solid line. The reduced 129 cm data do not show deviations from the  $1/v$  line that are not expected from resolution considerations.

The resonances reported by Flerov<sup>10</sup> to exist at 0.2 ev and in the region 0.5 to 0.9 ev have not been found. Even though these energy values, especially the latter, lie in a part of the spectrum that is poorly resolved, it can be said that if either of these resonances contributed more than, for example, 25 per cent, to the total cross section over an energy range corresponding to one detecting interval, its existence probably would have been indicated. Flerov based his conclusions on the difference between the ratios of cross section for 90°K neutrons to cross section for 290°K neutrons as observed for boron (assumed to be a  $1/v$  absorber) and for mercury. Bethel<sup>14</sup> and Kimura<sup>16</sup> suggest a resonance at from -0.3 ev to -0.1 ev. This would mean that the cross section would go up faster than  $1/v$  as  $v$  approaches zero. Such a trend is not observed.

The average cross section of mercury for the entire 300°K distribution of neutrons as determined from the summation of the observed data is  $376 \pm 4 \times 10^{-24}$  sq cm. This value is in satisfactory agreement with the value of  $430 \times 10^{-24}$  sq cm found by Dunning et al.<sup>15</sup> There are several reasons why the present determination may be expected not to agree with other determinations exactly. Work of an exploratory nature done in this laboratory previously indicates that for a larger mass of paraffin around the target than that used in the present experiments the distribution is shifted somewhat toward lower velocities. This fact indicates that the shape and size on the slow neutron source can have an appreciable effect on the average cross-sectional determinations (although they will not influence the spectrometer results if resolution corrections are made). Second, it has been observed by the author that there are relatively more very slow neutrons produced if the beam pulse is lengthened. This is due in part to the resolution effects: nevertheless it suggests that as a steady-state condition is reached in the slowing process, the very slow neutrons probably increase in relative abundance. Average cross sections determined under steady-state conditions (the conditions generally

prevailing for such determinations) would then be greater than the present value. Finally, the geometry of the experiment must be taken into consideration.

The resolution corrections do not have a very profound effect on the cross-sectional data for mercury. Upon examining the detector response curves, however, it is found that the conclusions obtained depend rather sensitively on the corrections applied. That this is the case may be seen by examining the curves "Observed I" and "Observed II" in Fig. 8. As was explained in Sec. 5, the former is the velocity distribution deduced, assuming a certain variation of the half-life of decay of delayed emission neutrons with the neutron velocity; the latter is the distribution required to explain the observed detector response if it is assumed that neutrons of all velocities rise and decay in intensity at the source with the same period. The difference in the shape of these two curves emphasizes the desirability of knowing the source time-velocity characteristics in as much detail as is possible. It is regrettable that time limitations precluded further experimental investigation. However, even a casual examination of the data presented in Fig. 5 shows that the constant half-life assumption can be only a rough approximation of the truth and that the present treatment, although it leaves much to be desired, is a step in the right direction. The curve "Observed I," therefore, is probably not too far from the true distribution, and, in spite of the uncertainties, several conclusions concerning it may be drawn.

The  $400^{\circ}\text{K}$  Maxwellian distribution shown on the same plot as the above curves is probably the best fit that could be found for either curves I or II, i.e., the best Maxwellian fit. There is an excess of fast neutrons in the (either) observed distribution compared not only to a Maxwellian for the temperature of the paraffin at the source ( $300^{\circ}\text{K}$ ), but there is such an excess compared to a  $400^{\circ}\text{K}$  distribution (both Maxwellians being "fit" to the slow side of the observed distribution). Such an excess of fast neutrons is to be expected because of the presence of the "cascading" neutrons of those being slowed down but not yet in even approximate thermal equilibrium. Bethe<sup>13</sup> shows that at neutron energy  $E \sim 8\text{keV}$  the Maxwell distribution and the cascade distribution should make equal contributions to the total distribution. If  $T$  is taken as  $400^{\circ}\text{K}$ , this energy corresponds to a velocity of approximately  $7\text{ km/sec}$  as calculated and to  $6.4\text{ km/sec}$  as observed. Inasmuch as it is not clear what taking  $T$  as  $400^{\circ}\text{K}$  means, this agreement may be fortuitous.

The detector response curves shown in Fig. 6 show a decided shift of the distribution to lower velocities with lower temperature. Resolution corrections were not applied to these data to obtain the velocity distribution curves; however, estimates were made of the positions of the maxima of such curves. From these estimates it was found that the distribution from the dry-ice - cooled ( $200^{\circ}\text{K}$ ) source approximates a Maxwellian for  $300^{\circ}\text{K}$ , and that the distribution from the liquid-air - cooled ( $135^{\circ}\text{K}$ ) source is roughly similar to a  $250^{\circ}\text{K}$  Maxwellian.

One reason for investigating cold source was to find out whether the velocity spectrum is much enriched in the slow-velocity end. Such a source is desirable in cross-sectional determinations in which data must be taken for a long time in order to obtain reasonable statistics in the last few time intervals. The curves as plotted in Fig. 6 are adjusted in order to have the same area under each of them; however, they represent the absolute

Table 6--Data Taken at 129 cm. Times are the same as in Table 5. In This Table, as in the One above, All Corrections Have Been Applied to the Data

	Time interval									
	1	2	3	4	5	6	7	8	9	10
$N_0(\text{net})$	2856	4022	6739	6978	5454	3168	1977	1246	877	559
$N_{\beta}(\text{net})$	2329	2496	3450	2895	1753	938	524	360	122	81
1/T	1.23	1.61	1.95	2.41	3.11	3.31	3.77	3.47	7.2	6.9
Mean error	0.09	0.07	0.06	0.07	0.12	0.23	0.41	0.53	3.1	4.3

Table 7--Data for the Dry-ice - cooled Source ( $200^{\circ}\text{K}$ ). Uncorrected for slow Neutrons from Previous Cycle. Times are same as in Tables 5 and 6.  $d = 248.5$  cm

	Time interval							
	1	2	3	4	5	6	7	8
$N_0(\text{net})$	766	915	994	1225	1730	2127	1927	1570
Mean error	137	92	82	84	91	60	58	55

	Time interval						
	9	10	11	12	13	14	15
$N_0(\text{net})$	1233	981	725	600	443	335	286
Mean error	52	51	58	56	55	51	45

Table 8--Data for Liquid-air - cooled Source ( $135^{\circ}\text{K}$ ). Uncorrected for Slow Neutrons from Previous Cycle. 320-Microsecond Sensitive Intervals. Other Times as in Tables 5, 6, and 7.  $d = 248.5$  cm

	Time intervals						
	1	2	3	4	5	6	7
$N_0(\text{net})$	1650	2118	2883	2543	1708	1120	880
Mean error	156	71	73	71	41	33	108

#### ACKNOWLEDGEMENTS

The author wishes to express his gratitude to Professor J. H. Manley, director of this research, for helpful advice and cooperation throughout the progress of this work. He is indebted also to Professor L. J. Haworth and to F. N. Gillette for design and construction of part of the equipment used in this investigation and to the latter for cooperation in some of the experimental work. The author wished to thank Professor M. Goldhaber who

kindly consented to oversee the final stages of the work in the absence of Professor Manley. The financial support of the Graduate School Research Board for equipment used in this research is also acknowledged.

#### REFERENCES

1. Dunning, Pegram, Fink, Mitchell, and Segre, *Phys. Rev.*, 48: 704 (1935); *Phys. Rev.*, 49: 103 (1936); Fink, *Phys. Rev.*, 50: 738 (1936).
2. L. W. Alvarez, *Phys. Rev.*, 54: 609 (1938).
3. Fertel, Gibbs, Moon, Thomson, and Wynn-Williams, *Proc. Roy. Soc.*, 175: 316 (1940); *Nature*, 142: 829 (1938).
4. C. P. Baker and R. F. Bacher, *Phys. Rev.*, 59: 332 (1941).
5. L. J. Haworth, J. H. Manley, and E. A. Luebke, *Rev. Sci. Instruments*, 12: 591 (1941).
6. E. A. Luebke, Ph.D. Thesis, University of Illinois, Urbana (1941).
7. J. H. Manley, L. J. Haworth, and E. A. Luebke, *Rev. Sci. Instruments*, 12: 587 (1941).
8. L. J. Haworth, *Rev. Sci. Instruments*, 12: 478 (1941).
9. F. N. Gillette, Ph.D. Thesis, University of Illinois, Urbana (1942).
10. Flerov, *J. Exp. Theoret. Phys. (U.S.S.R.)*, 9: 143 (1939).
11. H. A. Bethe, *Rev. Mod. Phys.*, 9: 139, 149 (1937).
12. H. A. Bethe, *op. cit.*, e.g., p. 149 [see also Dunning et al., *Phys. Rev.*, 47: 888, 796 (1935)].
13. H. A. Bethe, *op. cit.*, p. 126.
14. H. A. Bethe, *op. cit.*, p. 149.
15. Dunning, Pegram, Fink, and Mitchell, *Phys. Rev.*, 47: 416 (1935).
16. M. Kimura, *Phys. Rev.*, 60: 688 (1941).

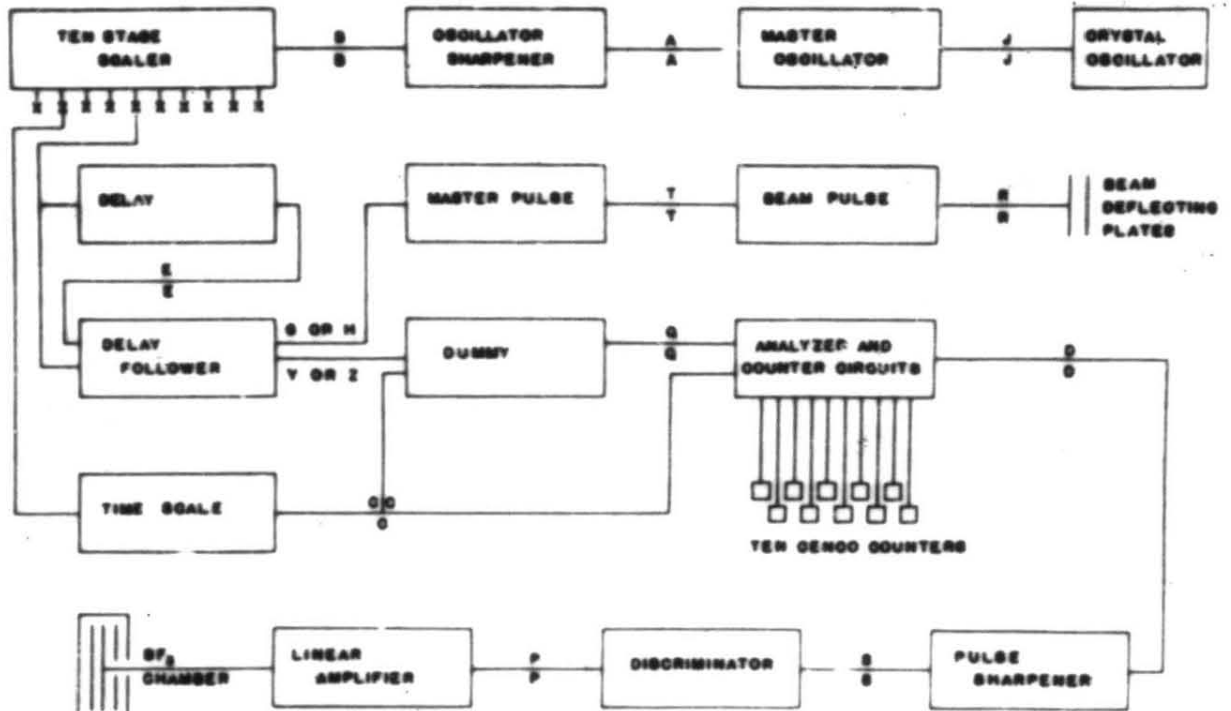


Fig. 1--Block diagram of the modulating, detecting, and analyzing circuits.

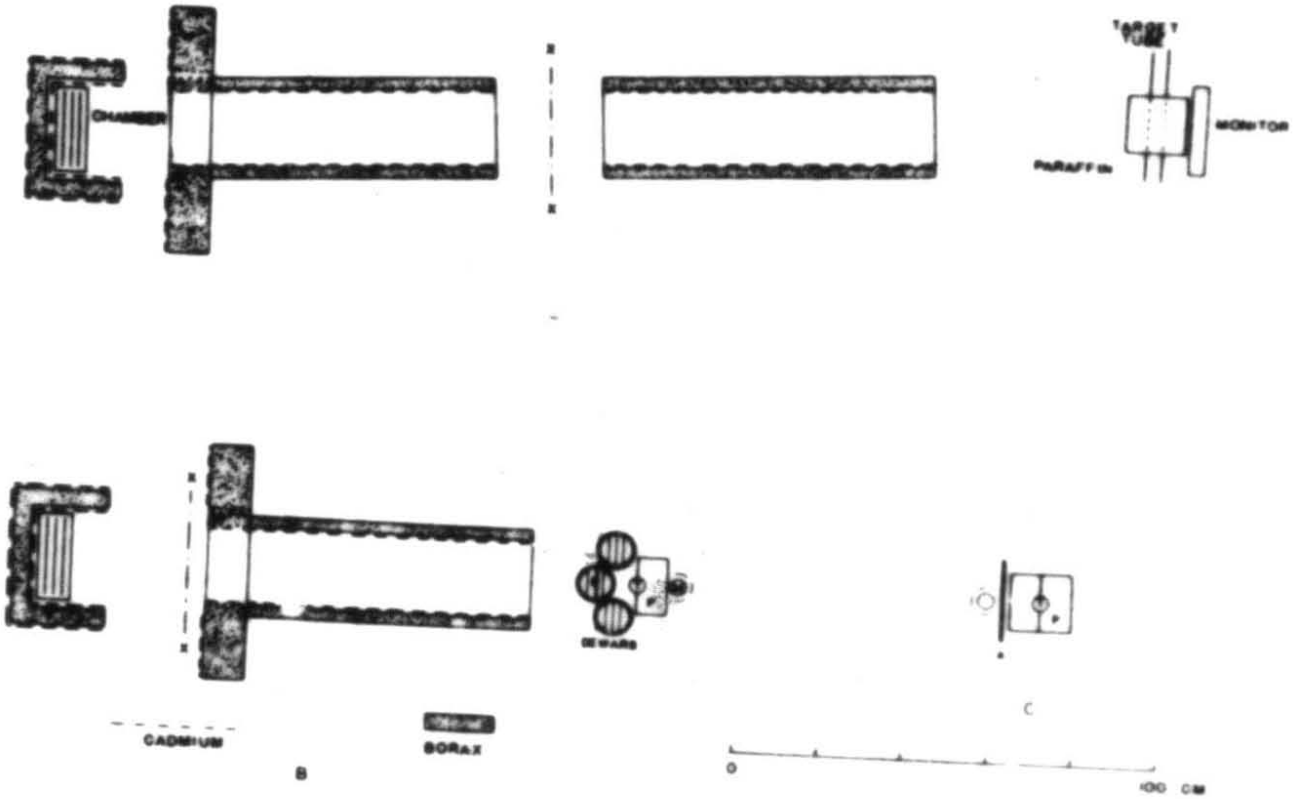


Fig. 2--Geometrical arrangement of the source, detector, and shielding.